

# Solutions to Problem Set 11

Fundamentals of Simulation Methods 8 ECTS  
Heidelberg University WiSe 20/21

Elias Olofsson  
ub253@stud.uni-heidelberg.de

February 8, 2021

## 1 Isothermal 1D hydrodynamics solver: sound pulse (7 pts)

Here in this problem, we use the 1D finite-volume solver implemented in the previous problem set, for another 1D isothermal hydrodynamics problem. This time, we specify the domain to  $x \in [-1, 1]$  and divide it into  $N = 100$  equally sized cells. Using periodic boundary conditions and setting the isothermal speed of sound to  $c_s = 1$ , we adopt the initial conditions

$$\rho(x, t = 0) = 1 + \epsilon \exp\left(-\frac{x^2}{2\sigma^2}\right), \quad (1)$$

$$u(x, t = 0) = 0, \quad (2)$$

with magnitude  $\epsilon = 10^{-4}$  and standard deviation  $\sigma = 0.2$  for the initial Gaussian density perturbation. For this simulation we specify the CFL-parameter to 0.4. Using the intuition we established from the previous problem set, we would expect the initial density perturbation to propagate out towards the edges of the domain. The two waves will have opposite velocity but same speed, and due to the periodic boundary conditions, will loop around at the edges and continue to transverse the domain. By solving the system and integrating in time up to  $t_{\max} = 2.0$  we can plot the density evolution in a  $xt$ -diagram, as seen in Fig.(1). For implementation specific details, please reference the attached Jupyter Notebook `fsm_ex11_eliasolofsson.ipynb`.

Here in this figure, we can confirm our initial beliefs and study how two waves propagate in opposite directions within the domain. Furthermore, we can estimate the sound crossing time scale to  $t_{c_s} = 2$ , since this is the time it takes for the sound waves to reach the initial position again. This result makes sense, since we specified the sound speed to  $c_s = 1$  and with the length of the domain being  $L = 2$ , we would expect  $t_{c_s} \approx \frac{L}{c_s}$ .

We can solve the same system again for an increased integration time of  $t_{\max} = 10 \cdot t_{c_s} = 20$  to study the system at the times  $t^* = n \cdot t_{c_s}$  for  $n \in \{0, 1, \dots, 10\}$ , i.e. at multiples of the sound crossing time. Solving the

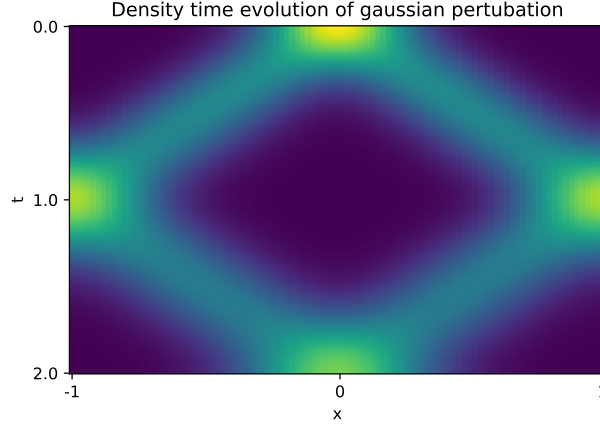


**Figure 1** – Density time evolution shown in a  $xt$ -diagram, for times  $t \in [0, 0.2]$  for the entire domain  $x \in [-1, 1]$ . Yellow color signifies high density, while blue corresponds to low density.

system for the increased integration time  $t_{\max}$ , for CFL-parameters 0.4 and 1.0, we can plot and compare the density profiles at times  $t^*$ , as well as the  $xt$ -diagrams for the full density evolution. The results obtained can be seen in Fig.(2).

For the CFL = 0.4 case, we can see how heavily the numerical diffusion is affecting the solution over time. Kinetic and potential energy are with time converted into "heat" through the numerical diffusion present in the simulation, which leads to an effective dampening of the system. However, as discussed in previous problem sets, by setting the CFL-parameter to precisely 1.0, we can largely stop the numerical diffusion for this particular simulation. As a result, we can not see any apparent decrease in magnitude or increase in standard deviation for the initial wave in the graph.

To verify these conclusions, we calculate and plot the time evolution for the total kinetic energy of the system, for both cases of 0.4 and 1.0 for the CFL-parameter. The results can be seen in Fig.(3).

Here in this figure, we can clearly see the gradual decrease in kinetic energy of the system, which aligns with the observed dampened behaviour in the density evolution of Fig.(2). Similarly, we can visually not see any apparent decline in kinetic energy for the case with CFL = 1.0 within the current time frame, which also corresponds to the observed behaviour in Fig.(2).

We repeat this entire simulation for an increased grid resolution  $N = 1000$ , and plot the resulting density evolution comparison in Fig.(4) and the corresponding total kinetic time evolution in Fig.(5).

Here we can notice that by increasing the grid resolution, we effectively reduce the effect of the numerical diffusion in the simulation. Still, best

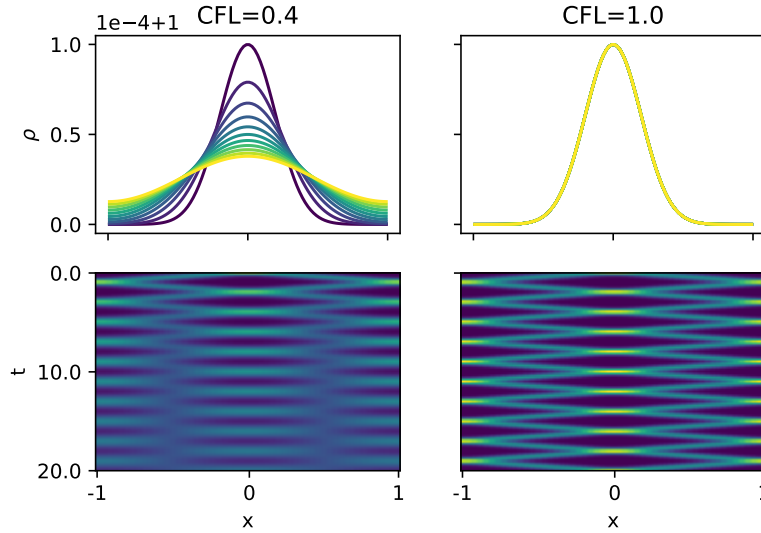


**Figure 2** – Top row: density profiles  $\rho(x, t)$  for the entire 1D domain  $x \in [-1, 1]$  and for times  $t^* = n \cdot t_{cs}$  where  $t_{cs} = 2$  is the sound crossing time scale, and  $n \in \{0, 1, \dots, 10\}$ . Bottom row:  $xt$ -diagram for the density evolution  $\rho(x, t)$ , for the entire domain in  $x$  and times  $t \in [0, 20]$ . Left column corresponds to a CFL-parameter specified to 0.4, and the right column to CFL = 1.0. All simulations were performed with a grid resolution of  $N = 100$  cells.

reduction in effective numerical diffusivity is obtained by selecting CFL = 1.0.

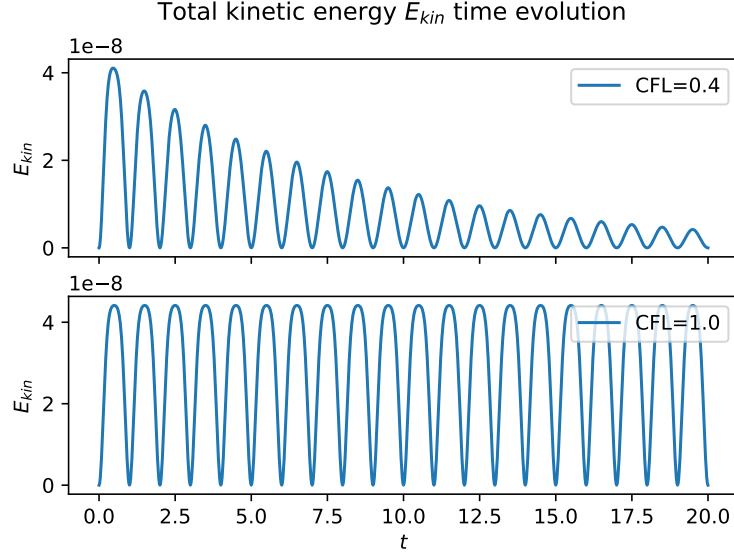


**Figure 3** – Time evolution of the total kinetic energy of the system, for time period  $t \in [0, 20]$ . Upper sub-figure corresponds to a CFL-parameter specified to 0.4, and with the lower being specified to 1.0. Both simulations were performed with a grid resolution of  $N = 100$ .

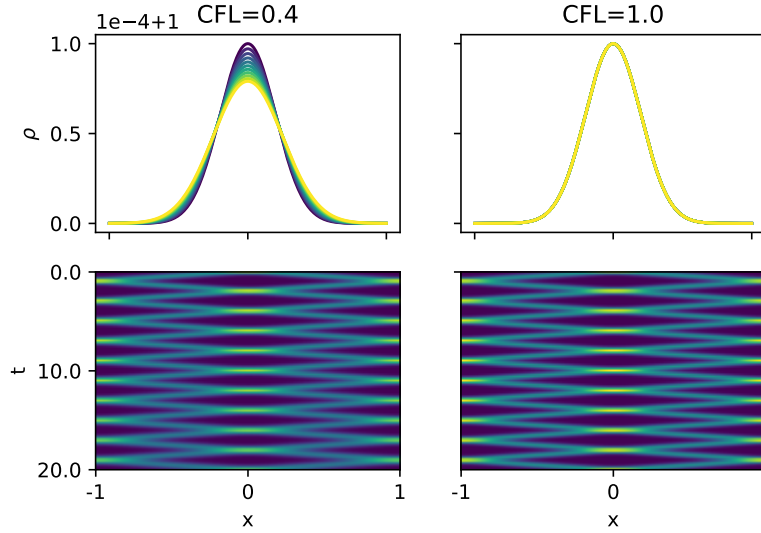


**Figure 4** – Top row: density profiles  $\rho(x, t)$  for the entire 1D domain  $x \in [-1, 1]$  and for times  $t^* = n \cdot t_{cs}$  where  $t_{cs} = 2$  is the sound crossing time scale, and  $n \in \{0, 1, \dots, 10\}$ . Bottom row:  $xt$ -diagram for the density evolution  $\rho(x, t)$ , for the entire domain in  $x$  and times  $t \in [0, 20]$ . Left column corresponds to a CFL-parameter specified to 0.4, and the right column to CFL = 1.0. All simulations were performed with a grid resolution of  $N = 1000$  cells.

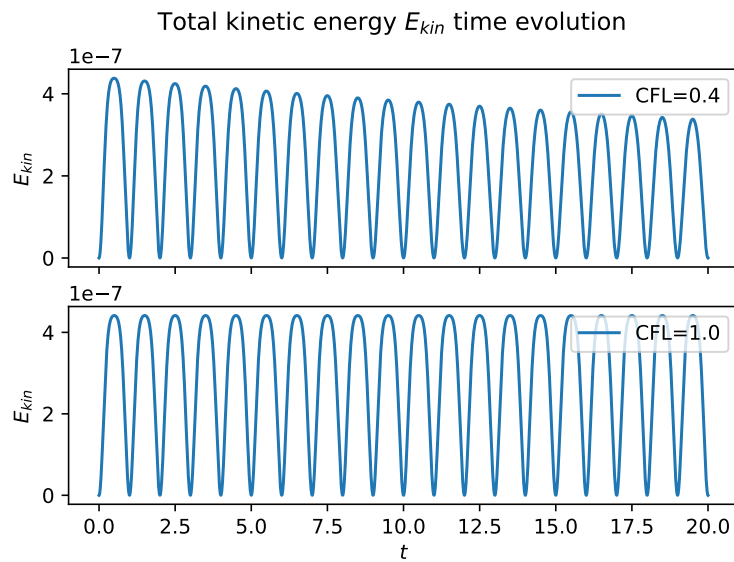


**Figure 5** – Time evolution of the total kinetic energy of the system, for time period  $t \in [0, 20]$ . Upper sub-figure corresponds to a CFL-parameter specified to 0.4, and with the lower being specified to 1.0. Both simulations were performed with a grid resolution of  $N = 1000$ .

## 2 1D Euler Riemann problem (13 pts)

In the next problem, we build upon our previous finite-volume solver to adopt it to the Euler Riemann problem. Now, we specify the conservative variables to

$$\mathbf{q} = \begin{bmatrix} \rho \\ \rho u \\ \rho E \end{bmatrix}, \quad (3)$$

with the Euler flux function as

$$\mathbf{F} = \begin{bmatrix} \rho u \\ \rho u^2 + P \\ u(\rho E + P) \end{bmatrix}, \quad (4)$$

where  $\rho E$  is the total energy density, given as

$$\rho E \equiv e_{\text{int}} + \frac{\rho u^2}{2}, \quad (5)$$

where  $e_{\text{int}}$  is the internal energy density. For our specification of the physical fluxes, the equation of state is adiabatic. Thus we can close the system by relating the pressure  $P$  as per

$$P = (\gamma - 1)e_{\text{int}} = (\gamma - 1) \left( \rho E - \frac{\rho u^2}{2} \right), \quad (6)$$

where  $\gamma$  is the adiabatic index and which we for this simulation set to 1.4. Differing from the previous simulations, we will not have a constant and uniform speed of sound in this simulation. Instead, we will at each cell center (and by constant reconstruction to the left/right sides of each cell interface) estimate the local sound speed as

$$c_s \equiv \sqrt{\frac{\gamma P}{\rho}}. \quad (7)$$

We also adopt the initial conditions

$$\rho(x, 0) = \begin{cases} 1 & \text{for } x \leq 0.5 \\ 0.125 & \text{for } x > 0.5 \end{cases}, \quad (8)$$

$$P(x, 0) = \begin{cases} 1 & \text{for } x \leq 0.5 \\ 0.1 & \text{for } x > 0.5 \end{cases}, \quad (9)$$

$$u(x, 0) = 0, \quad (10)$$

with Dirichlet boundary conditions defined by the initial conditions at the boundaries.

We solve the problem at hand and integrate in time to  $t_{\max} = 0.2$ , and plot the density  $\rho(x)$ , velocity  $u(x)$  and pressure  $P(x)$  profiles at the final state, as well as the time evolution of the density in a  $xt$ -diagram. The results can be observed in Fig.(6). For implementation specific details, please reference the attached Jupyter Notebook `fsm_ex11_eliasolofsson.ipynb`.

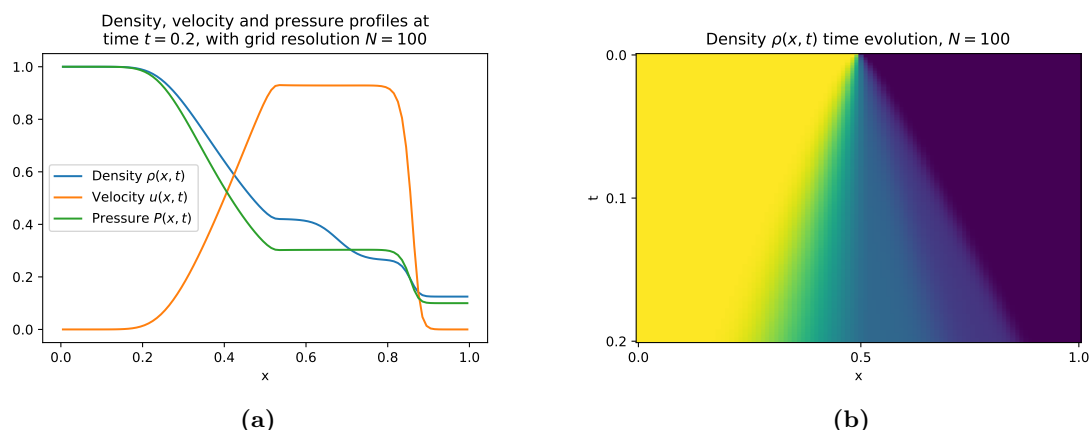


**Figure 6** – Solution of the 1D Euler Riemann problem, with grid resolution  $N = 100$ , and initial conditions given by Eq.(8-10). Left: density, velocity and pressure profiles within the domain  $x \in [0, 1]$ , at the final simulated time  $t = 0.2$ . Right:  $xt$ -diagram of density evolution  $\rho(x, t)$ , for the entire domain  $x \in [0, 1]$  and for time  $t \in [0, 0.2]$ . Yellow color signifies high density, while blue corresponds to low density.

Here we can see how the initial discontinuity forms a shock wave, traversing the domain to the right in the figure at constant speed. Behind the shock wave, we can discern the contact discontinuity slowly trailing behind, also to the right, marking the remains of the original boundary between the two initial fluid phases. Travelling in the other direction, to the left in the picture, we have the rarefaction wave signifying the region where the fluid expands due to a positive velocity gradient, which in turn yields a smooth negative gradient of the density and the pressure. Thus the rarefaction region is more of a "fan" rather than a "wave", since it is so spatially elongated.

We increase the grid resolution to  $N = 1000$  and solve the same problem again, with the same parameters and initial conditions. The results can be seen in Fig.(7).

As expected, the solution becomes much sharper and more distinct, due to the decreased effective numerical diffusivity. Since diffusion tends to have a smoothing effect on the solution, when we increase the grid resolution, shock waves and other characteristics are asymptotically approaching their analytical counterparts, where e.g. shocks and contact discontinuities are perfect and exact discontinuities.

Playing around with the initial conditions, we find that if we set the

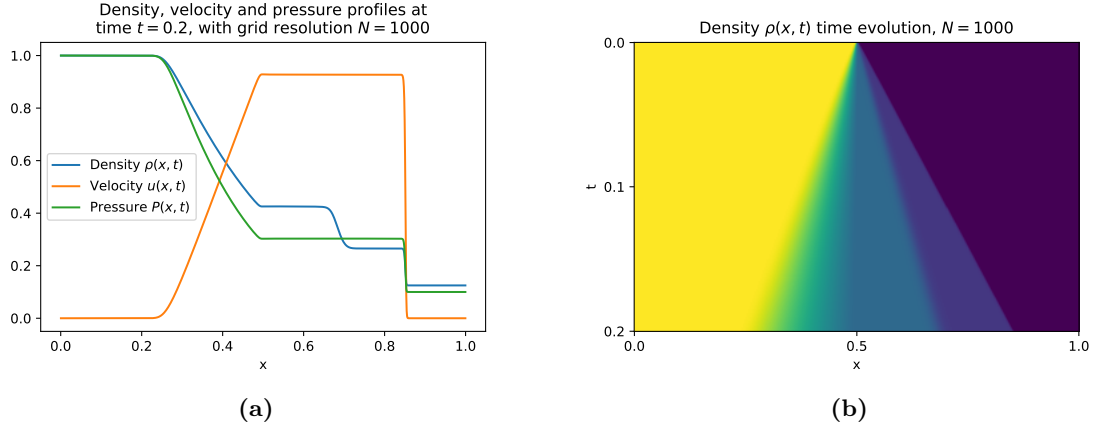


**Figure 7** – Solution of the 1D Euler Riemann problem, with grid resolution  $N = 1000$ , and initial conditions given by Eq.(8-10). Left: density, velocity and pressure profiles within the domain  $x \in [0, 1]$ , at the final simulated time  $t = 0.2$ . Right:  $xt$ -diagram of density evolution  $\rho(x, t)$ , for the entire domain  $x \in [0, 1]$  and for time  $t \in [0, 0.2]$ . Yellow color signifies high density, while blue corresponds to low density.

symmetrical initial conditions

$$\rho(x, 0) = \begin{cases} 1 & \text{for } |x - 0.5| \leq 0.2 \\ 0.125 & \text{for } |x - 0.5| > 0.2 \end{cases}, \quad (11)$$

$$P(x, 0) = \begin{cases} 1 & \text{for } |x - 0.5| \leq 0.2 \\ 0.1 & \text{for } |x - 0.5| > 0.2 \end{cases}, \quad (12)$$

$$u(x, 0) = 0, \quad (13)$$

where a region of high pressure and density are centered at  $x = 0.5$  with a width of 0.4. Solving this system with these initial conditions, we obtain the results shown in Fig.(8).

Here we have two shock waves, travelling in opposite directions towards the domain boundaries. We also have two contact discontinuities trailing behind each shock wave, and two rarefaction fans travelling towards the center and eventually merging together at the end of our simulation.



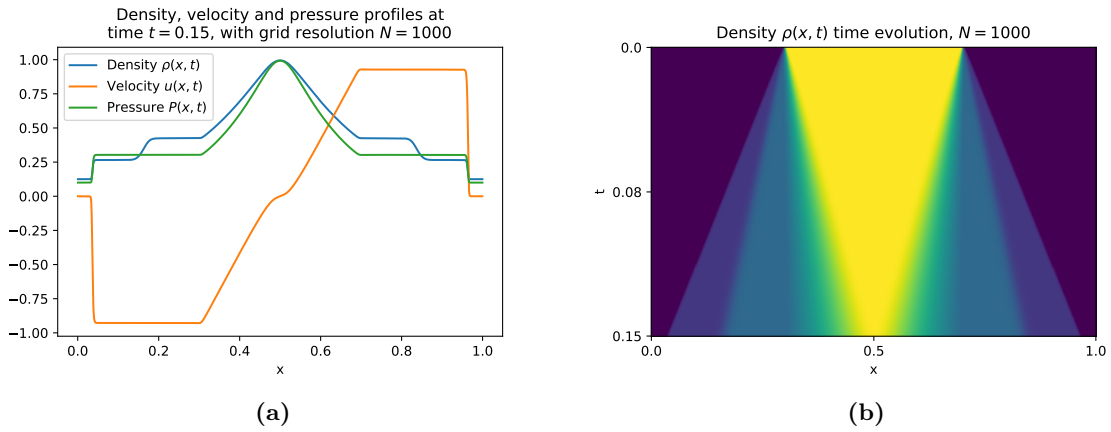


**Figure 8** – Solution of the 1D Euler Riemann problem, with grid resolution  $N = 1000$ , and initial conditions given by Eq.(11-13). Left: density, velocity and pressure profiles within the domain  $x \in [0, 1]$ , at the final simulated time  $t = 0.15$ . Right:  $xt$ -diagram of density evolution  $\rho(x, t)$ , for the entire domain  $x \in [0, 1]$  and for time  $t \in [0, 0.15]$ . Yellow color signifies high density, while blue corresponds to low density.